Title: Insight Mechanistic of Hydroxychloroquine on Ventricular Myocytes and Tissue in COVID-19 and Common Comorbidities: An In-silico perspective

Short Title: In-silico Ventricular model of COVID-19 and HCQ

Author Information:

Ponnuraj Kirthi Priya

Scientist, Tata Consultancy Services Limited, Bangalore, India

Address: D-Block, Gopalan Global Axis, Rd Number 9, Opp Satya Sai Hospital, KIADB Export Promotion Industrial Area, Whitefield, Bengaluru, Karnataka 560066

E-mail: p.kirthipriya@tcs.com

Corresponding Author:

Srinivasan Jayaraman

Sr.Scientist, Tata Consultancy Services Limited, America

Address:Portland, Oregon, USA- 97229

Ph: +1-971 329 6916

E-mail: srinivasa.j@tcs.com

Insight Mechanistic of Hydroxychloroquine on Ventricular Myocytes and Tissue in COVID-19 and Common Comorbidities: An In-silico Perspective

In-silico Ventricular model of COVID-19 and HCQ

Ponnuraj Kirthi Priya [1] and Srinivasan Jayaraman*[2]

[1]*Scientist, Tata Consultancy Services Limited, Bangalore, India, p.kirthipriya@tcs.com*
[2]*Sr.Scientist, Tata Consultancy Services Limited,Portland, USA, srinivasa.j@tcs.com*

Abstract

Rationale: Several drugs have been attempted to treat SARS-CoV-2 (COVID-19), the global pandemic, of which Hydroxychloroquine (HCQ) shows a significant clinical outcome, irrespective of cardiotoxicity. Although few clinical observations have been reported in similar line, HCQ manifestation towards pro-arrhythmia has not been elucidated. This demands further investigation on the role of biological variability in its many forms in determining COVID-19 patient's responses to drugs.

Objective: To investigate HCQ interaction mechanistic under COVID-19 with and without pro-arrhythmic comorbidities such as Long QT syndrome (LQTS1 & 2), and hypokalemia in, (a) three types of cardiomyocytes (b) ventricular tissue and its effects when excited with premature beats (PBs) to understand the possibility of arrhythmogenesis.

Methods and Results: A 2D transmural anisotropic ventricular tissue model consisting of endocardial, midmyocardial and epicardial myocytes are configured for *mild* and *severe* COVID-19, comorbid and HCQ conditions. Results show that along with QT interval reduction, low amplitude and/or inversion T-wave occurred in *mild* and *severe* COVID-19 conditions respectively. In contrast, under LQTS1 with mild hypokalemia, leads to notched T-waves, and HCQ inclusion increases the QT interval and T-peak in all *mild* infections. *Severe* COVID-19 causes inverted T-waves and shorten QT-interval in all comorbidities except in LQTS2, where biphasic T-waves is observed. Arrhythmogenesis, reentry is created only on addition of *mild* hypokalemia while ST elevation is observed in presence of *moderate* and *severe* hypokalemia. When treated with HCQ, insignificant impact observed.

Conclusion: In-silico ventricular model indicates, HCQ has insignificant effect on COVID-19 with and without comorbidities, except in the combination of mild COVID-19 with moderate hypokalemia condition and *severe* COVID-19 with mild hypokalemia where it initiated a re-entrant arrhythmia. These results could guide towards COVID-19 management.

Keywords

Hydroxychloroquine, SARS-CoV-2, Hypoxia, Cardiotoxicity, Ventricular Arrhythmia, Hypokalemia

*corresponding author

1 Introduction

The novel Severe Acute Respiratory Syndrome Coronavirus (SARS-CoV-2), responsible for the COVID-19 pandemic, has become a major concern since it was first reported in Wuhan, China in December 2019. As of May 30, 6,033,469 cases have been reported worldwide with 366,890 deaths, efforts are being made worldwide to effectively screen, contain, diagnose and treat this virus[1]. Coronaviruses (CoVs) are single-stranded RNA viruses that have the ability to mutate and recombine rapidly. SARS-CoV-2 belongs to the β-CoVs group and binds to the zinc peptidase angiotensin-converting enzyme 2 (ACE2) to enter the host cell. Suppression of ACE2 expression changes the pathology of lungs and contributes to severe pneumonia and acute lung failure observed with this virus[2]. Onset of the illness is identified through common symptoms like fever, cough and shortness in breathing. Other less occurring symptoms are muscle pain, anorexia, malaise, sore throat, nasal congestion, dyspnea and headache. These symptoms typically appearing 2-14 days after exposure. Real-time polymerase chain reaction (RT-PCR) test of nasopharyngeal and oropharyngeal samples is currently the gold standard for confirming the presence of COVID-19. Further, chest X-rays and computed tomography (CT) scans are being explored to detect and assess COVID-19 patients through deep learning[3,4]. CT of lungs of patients show bilateral patchy shadows or ground glass opacity.

Several antiviral drugs[5] that had been used to treat SARS-CoV1 and Middle East Respiratory Syndrome (MERS-CoV) were attempted for treating SARS-CoV-2, albeit with an inconsistent efficacy. Notable therapeutic antimicrobials that are currently being explored and have exhibited positive inhibitory effect for treatment of COVID-19 are chloroquine (CQ), hydroxychloroquine (HCQ) (both targeting prevention or treatment of malaria), HCQ with azithromycin, lopinavir/ritonavir[6], (used during SARS & MERS outbreak) and Remdesiver(GS-5734), which showed promising outcome during Ebola virus outbreak. Among these, CQ has been declared as a highly promising drug for COVID-19 according to the 6th edition of new coronavirus pneumonia diagnosis and treatment plan, released by National Health and Care Commission of China (Feb 19 ,2020). An in-vitro study reported the potential activity of HCQ on SARS-CoV-2[7]. Although HCQ, an antirheumatic drug[8,9], has a similar chemical structure to CQ, in-vitro studies[7] showed HCQ is more potent in inhibiting SARS-CoV-2 ; interested readers could refer[10,11] for more details on the effect of HCQ in preventing infection and disease progression. Subsequently, the negligible cost and known safety profile of this drug has been considered for SARS-CoV-2 treatment. To date, there is no clinical evidence that provides the detailed mechanism of HCQ's safety or adversity on SARS-CoV-2 infection, in particular, the cardiac cell and tissue level. To be specific, under what scenarios the target drug interaction may cause side effect or arrhythmia on a virus infected patient.

Findings from previous studies suggest that long-term (over 5 years) intake of HCQ is likely to contribute to the development of retinopathy, including QRS widening, QT interval prolongation, ventricular arrhythmia like Torsades de pointes (TdP), hypokalemia and hypotension[8,9]. However, its effect on COVID-19 infected individuals is not clear, leaving a scope for investigation. On a positive note, in experiments performed on mouse atria, Capel et al.[12] reported that HCQ acts as a

bradycardiac agent (reducing the spontaneous beating rate) in sinoatrial cells via a dose-dependent reduction of multiple ionic currents: 'funny' current (I_f), L-type calcium current (I_{CaL}) and rapid delayed rectifier potassium current (I_{Kr}). Modelling of drug cardiotoxicity at the cellular level focuses predominantly on reducing I_{Kr} current, which will inturn prolong the APD in cells and QT interval in whole heart level, thereby leading to arrhythmias like TdP[13]. However, a clinical study in France[14] reported that either HCQ alone or in combination with azithromycin (AZM) is efficient in treating COVID-19. Wang et al. reported that using a combination of HCQ and AZM for treating COVID-19 elicited electrical alternans, re-entrant circuits and wave breaks[15]. Azithromycin is an antibiotic drug that inhibits I_{Kr} current thus acting as a proarrhythmic agent[16]. However, Sarkar et al., 2012[17] reported that one population of cell differs from another (i.e healthy vs diseased) and electrophysiological variability manifests at every level, from molecular, cellular, organ, and organisam level. Hence, considering the outcome of previous clinical evidence of HCQ on normal cells may be inadequate to provide the exact impact of the effect of HCQ on SARS-CoV-2 cells or tissue.

In the present scenario, numerous research and clinical observations have reported important manifestations of COVID-19, including those of cardiac injury. For instance, common comorbidities observed in patients in United States were hypertension (14.9%), diabetes (7.4%) and coronary heart disease (2.5%). Complications observed were acute respiratory distress syndrome (ARDS) and septic shock in 3.4% and 1.1% respectively.[18]. Among the 44,672 patients studied in China, 4.2% were reported to have cardiovascular diseases (CVD) and 12.8% had hypertension. In this population, 80.9% were reported to have mild disease with no mortality, 13.8% had severe disease with no mortality, and 4.7% had critical disease with a case fatality rate of 49%. Though the percentage of patients with CVD was 4.2%, they included 22.7% of all fatal cases[19]. Yet, another study of 138 chinese COVID-19 patients, 26.1% had complications and had to be transferred to the ICU, including ARDS (61%), arrhythmias (44%) and shock (31%)[20]. Huang et al. reported that of the 41 patients admitted, the most common complications were ARDS (29%), viremia (15%), acute cardiac injury determined by elevated high-sensitivity troponin (12%), and secondary infection (10%)[21]. Another study[22] of 191 patients showed that fatality of the patients increased in presence of comorbidities like hypertension (48%), diabetes (31%) and coronary heart disease (24%) and non-survivors had higher rates of heart failure and acute cardiac injury than survivors. In China, the clinical characteristics of 1099 COVID patients was delineated[21,23]. Similarly, in Italy, Henry et al.[24] examined 33 laboratory parameters of 3377 patients and reported a significant increase in inflammatory biomarkers of cardiac and muscle injury, liver and kidney function and coagulation measures. Lymphopenia, prolonged prothrombin time and elevated lactate dehydrogenase was also reported. Further, the potassium concentration in blood was reported to be 3.9 (3.6-4.2) mmol/liter and 3.8 (3.5 to 4.1) mmol/liter in non-severe and severe COVID-19 patients respectively.

As our particular interest is in the human cardiac system; specifically electrophysiology, we wish to emphasis the variability of COVID-19 in cardiac system. Guo et al.[25] reported that among 187 COVID-19 patients, those with myocardial injury (elevated troponin T levels) led to fatal outcomes in comparison with those with underlying cardiovascular diseases including hypertension,

coronary heart disease and cardiomyopathy. Furthermore, clinical observations reported by Mercuro et al.[26] shows the median baseline QTc was 455 ms in 90 COVID-19 patients. In presence of HCQ, it increased to 473 ms and in presence of HCQ and azithromycin, it reduced to 442 ms. Among those who received HCQ alone, 19% had QTc prolongation of 500 ms or more, 13% had a change in QTc of 60 ms or more and 1 case of Torsade de Pointes (TdP) was reported. Furthermore, CQ has been shown to prolong QT interval and decline the T-wave amplitude by acting on the inward-rectifying potassium current (I_{K1}) and has been suggested as a potential therapy for short QT syndrome (SQT3)[27]. Thus its very evident that investigating and understand the cardiac manifestation mechanism due to COVID-19 and during medication like HCQ drug is critical.

Another comorbidity observed in COVID-19 patients is hypokalemia. Li X et al., 2019 study on 175 patients with COVID-19 reported that 39 patients had severe hypokalemia (under 3 mmol/L), 69 had moderate hypokalemia (3-3.5 mmol/L) and 67 were normokalemia (over 3.5 mmol/L)[28]. In a case report of the electrocardiogram (ECG) recording of two COVID-19 patients, the first case presented a temporary SIQIIITIII morphology followed by reversible AV-block while the second case demonstrated ST-segment elevation (STE) followed by multi focal ventricular tachycardia. ACE2 which is highly expressed in hearts and lungs, is the functional receptor for coronavirus. Thus, He et. al[29] proposed that ACE-2 signalling pathways may play a role in cardiac injury while hypoxemia caused by COVID-19 may cause damage to myocardial cells. Severe hypoxemia occurring in lungs of COVID-19 patients has been linked to loss of lung perfusion regulation and hypoxic vasoconstriction[30]. Acute viral infections like that of COVID-19 have been known to cause type 1 or 2 myocardial infarction though the frequency of STE in these patients is unclear[31].

Although various researchers have attempted to study the current pandemic SARS CoV-2: it's inhibitory mechanism on human cells, symptoms, diagnosis and treatment, for the reasons noted, it is critical to zero down the effect of a drug and explain its response range. Such comprehensive study, either using in-vivo or clinical studies is difficult in a short span of time with present day technology, in this situation, computational models can help to elucidate and overcome the following aspects:

- The effect of SARS-CoV-2 on electrophysiological properties of ventricular myocytes and spatiotemporal changes in tissues and organ level
- Lack of clinical evidence that provides a detailed influence of HCQ on SARS-CoV-2 infected cardiac cell and tissue. For example: changes in ECG, mechanism and potential severity of ventricular arrhythmias like TdP
- Mechanistic understanding of HCQ on ventricular myocytes and tissues under other comorbid scenarios, such as long QT syndrome (LQTS type 1 and 2), and hypokalemia.

To address the above gaps, we develop a 2D transmural anisotropic ventricular tissue model framework that can help in primarily understanding the SARS-CoV-2 effect on the three types of ventricular myocytes: endocardial, midmyocardial and epicardial. This framework allows one to understand the cardiac cellular and subsequently tissue level mechanism, including the response

to pharmacological agents like HCQ. Here, two variations of COVID-19; *mild* and *severe* are explored. Secondly, it is understood that in co-morbidities like congenital LQTS1 and drug induced LQTS2 conditions, the presence of HCQ causes an additional prolongation of QT interval and is hence contraindicated. However, the percentage prolongation of QT interval is not quantified. Thus, in a two-dimensional anisotropic transmural tissue, HCQ is introduced in presence of LQTS 1 & 2 and pseudo ECGs are created to understand if it mimics the same effect as those observed in clinical scenarios. Further, the presence of these conditions in SARS CoV-2 is examined. Thirdly, hypokalemia (mild, moderate and severe) along with SARS CoV-2 case are introduced one at a time to understand its effect on cardiomyocytes and ventricular tissue; with and without HCQ. In each case, the variations in the QT interval and T-peak are captured. Finally, the tissue is excited with premature stimuli to analyse and determine under which of the above three conditions the tissue becomes pro- arrhythmic. Although earlier studies have established that HCQ induces QT prolongation, TdP arises only in certain scenarios. This study is an attempt to address the possibilities under which an arrhythmia is generated at the tissue level in presence of the above mentioned conditions.

2 Methods

2.1 Human Ventricular Cardiomyocyte Model and its Ion Channel Activities due to COVID-19 and Specific Comorbid Condition

The rise and fall of membrane potential in single cardiomyocytes is described by the Ten Tusscher (TP06) model[32]. A stimulus current of amplitude 52 μA is applied for 1 ms is used to excite the cell. The parameters of the model, tissue characteristics and integration scheme are elaborated in Supplementary-1. The change in cardiomyocyte's ionic current parameters under various configurations: COVID-19, LQTS1, LQTS2, and hypokalemia are listed in Table 1.

Table 1: Change in parameters for different conditions

Condition	Ionic Current	Change
HCQ[12]	I_{Kr}	35% reduction
	I_{CaL}	12% reduction
LQTS1[33]	I_{Ks}	50% reduction
LQTS2[34]	I_{Kr}	50% reduction
Mild Hypokalemia (Hypokalemia1)[28]	Extracellular potassium concentration (K_o^+)	85% reduction
Moderate Hypokalemia (Hypokalemia2)	K_o^+	55% reduction
Severe Hypokalemia (Hypokalemia3)	K_o^+	45% reduction
Mild COVID-19	$[ATP]_i$	5.5 mM
	$k_{0.5}$	0.125
Severe COVID-19	$[ATP]_i$	5 mM
	$k_{0.5}$	0.250

As COVID-19 has been linked to causing hypoxemia[29], which in turn leads to hypoxia, this condition was included in the cardiac myocytes by increasing intracellular ATP concentration

which would in turn lead to activation of an ATP sensitive potassium current. Using the formulation of Shaw and Rudy[35], ATP activated K^+ current is described by the following formula

$$I_{ATP} = G_{k,ATP} \frac{1}{1 + (\frac{[ATP]_i}{k_{0.5}})^H} (\frac{[K_o^+]}{5.4})^n (V_m - E_k) \quad (1)$$

where $G_{k,ATP}$ is the maximum conductance of I_{ATP} current and has a value of 3.9 nS/cm^2, H and n have a value of 2 and 0.24 respectively. The intracellular ATP concentration ($[ATP]_i$) under normal condition is 6.8 mM, but it decreases to 5.5 mM in mild hypoxia and 5 mM in severe hypoxia respectively. Similarly, $k_{0.5}$ is 0.042 for normal condition, 0.125 and 0.25 for mild and severe hypoxia respectively[36]. Henceforth, in this study, hypoxia condition would be referred as COVID-19.

2.2 Two Dimensional Ventricular Cardiac Tissue Model

We build the 2D anisotropic transmural ventricular model[37]. Here, the depolarisation and repolarisation patterns generated from the tissue are validated by simulating pseudo ECGs based on the equations given by Gima & Rudy[38], readers looking for basics and more details may refer to Supplementary-1. Later, to investigate the benefits and adverse effects of HCQ under control, COVID-19 and other comorbid pathologies such as LQTS1, LQTS2 and hypokalaemia, the ion channel variations corresponding to these conditions were included in the cells of the tissue one at a time. A regular pacing pulse is applied in the tissue, and the corresponding voltage propagation is analyzed. Further, pseudo ECGs are generated for each of the clinical conditions. The variation in the ECG, in particular the QT interval and T-wave morphology are captured for analysis. Furthermore, the tissue is stimulated with premature stimuli in between the normal beats to study the conditions that can initiate or sustain an arrhythmia.

3 Numerical Results

3.1 Change in Cardiomyocytes Ionic Current and its Quantitative Contribution towards Action Potential

To understand the cellular mechanism of the three different types of cardiomyocytes such as endocardical (endo), M (mid) and epicardial (epi) cells, the action potential (AP) is generated under control, COVID-19 conditions as well as in presence of comorbidities like LQTS1, LQTS2, and hypokalemia. Further, the effect of HCQ is included in the cells in each of the above scenarios by reducing the I_{Kr} and I_{CaL} current. As an evaluation metric, the AP parameters: 1) action potential duration at 90% repolarization (APD_{90}) and 2) peak plateau potential values of the three types of cells under different scenarios are captured and tabulated in Table 2.

3.1.1 Effect of HCQ in Control and COVID-19 Infected Cardiomyocytes

Fig. 1(i-iii) shows the APs between normal and HCQ condition in the three cell types. It has been observed that the prolongation of the action potential duration (APD) in M-cells is 6.72% (23.944 ms), higher than that of endo (2.87% (7.989 ms)) and epi cells (2.93% (7.982 ms)) due to the decrease in I_{Kr} current. In contrast, it is observed that the plateau phase peak is slightly decreased by 4.69% (1.65), 5.01% (1.83) and 4.97% (1.81) in endo, mid and epi cells respectively due to the reduction of I_{CaL} current.

The AP generated in *mild* and *severe* COVID-19 conditions in all three types of myocyte are shown in Fig. 1(iv-vi). Here, APD is reduced by 3.76%, 7.70% and 3.54% in *mild* COVID-19 and by 20.65%, 31.35% and 19.90% in *severe* COVID-19 in endo, mid and epi cells respectively. But, the plateau peak in comparison with control condition (all three cells) decreases by an average of 4.08% and 18.32% in *mild and severe* COVID-19 case respectively. On including HCQ for *mild* COVID-19, the APD slightly increases by 2.20%, 4.87% and 2.25% while the plateau peak got reduced by 4.89%, 5.76% and 5.25% in the endo, mid and epi cells respectively. Due to the reduced APD under *mild* and *severe* COVID-19 conditions, the cells come out of their refractory state sooner and are available for re-excitement, subsequently leading to the possibility of reentrant arrhythmia in ventricular tissue. To be specific, introduction of HCQ in *mild* COVID-19 causes the APD to prolong and reach near control values. A higher APD prolongation in mid cells is observed than other cell types. In contrast, under *severe* COVID-19, HCQ effect on APD is negligible (0.38%) while the difference in plateau peak is found to be 5.83%, 6.63% and 7.12% in endo, mid and epi cells respectively. This infers that under *severe* COVID-19 condition, HCQ has an insignificant effect either on APD or peak plateau potential in cardiomyocytes.

3.1.2 HCQ Effect on Cardiac Myocytes with Pre-existing Long QT Syndrome

***LQTS1 with COVID-19*:** In case of LQTS1, as a response to 50% reduction of the conductance of I_{Ks} current in the myocytes, it is observed that the APD is prolonged by about 15% in comparison to control in all three cell types and the peak of plateau phase is slightly higher, with a minor difference in the endo, mid and epi cells as shown in Fig. 1(vii-ix). When treated with HCQ, APD generate multiple early after depolarizations (EADs) in mid cells and returns to rest state at 838.37 msec. Delayed or early after depolarizations are also ventricular tachycardia mechanisms during ischemia[39]. Thus, the change in APD ($\triangle$APD) between control versus LQTS1 with HCQ infers a 20.44% (56.76 msec), 135.37% (482.19 msec) and 20.18% (54.852 msec) in endo, mid and epi cells respectively and the percentage difference in plateau peak in all cells is about 4.62%.

The combination of LQTS1 and *mild* COVID-19 prolongs the APD by 8.84% and 9.28% in endo and epi cells respectively, while the increase in mid cells is negligible. The peak plateau is reduced by 3.64%, 7.38% and 3.75% respectively in the endo, mid and epi cells. On adding HCQ, the APD increases by 12.6%, 7.65% and 12% and plateau peak decreases an average of 8.76% with respect to control. In contrast, when comparing with *mild* COVID-19, HCQ increases the APD in endo, mid and epi cells by 3.76%, 7.16% and 2.72% respectively.

In presence of LQTS1 and *severe* COVID-19, the decrease in mid cells APD (29.21%) is

higher than that of endo (14.96%) and epi (14.01%) cells, while the reduction in plateau peak is lower in mid cells (6.85%) than in endo (17.89%) and epi (18.40%). Result infers that APD has minimal change, while the reduction in plateau peak is an average of 23.54% in all cells, when comparing with control. While, LQTS1 infected with *severe* COVID-19 and treated with HCQ shows no significant effect.

***LQTS2 with COVID-19*:** In LQTS2, as a response to reducing the conductance of I_{Kr} current to 50% in the three cell types, the APD prolongation in mid cells is 25.46% higher (90.69 ms) in comparison to 7.47% in endo (20.75 msec) and 7% in epi (19.032 msec) cells as seen in Fig. 1(x-xii) and the difference in peak of plateau phase is about 1.09% in all the three cell types. This is slightly higher in comparison to LQTS1. As an effect of HCQ treatment, APD further extended by 8.55% in endo and epi cells. While in mid cells a single EAD is generated and later the AP returns to rest state at 657.97 msec, which is a change of APD ($\triangle$APD) of 84.72%(301.79 msec) comparing to control mid cell. But, the percentage difference in plateau peak ($\triangle$Plateau peak) is about 4% in all three cell types.

LQTS2 in combination with *mild* COVID-19 increases the APD by 3.15%, 6.75% and 3.18% in endo, mid and epi cells respectively; while the reduction in plateau peak is an average of 3.01% in all three cell types. On introducing HCQ, the APD increase in mid cells (9.35%) is higher than that of other cells (3.98%), but plateau peak decreases in mild cells (17.78%) than endo (7.99%) and epi (8.33%) cells with respect to control. When HCQ treated for COVID-19 mid cell's APD increases by 2.6% and plateau peak by 14.72%, which is very high comparing to endo and epi cell. However, HCQ impact or effect on LQTS2 infected with *mild* COVID-19 is lower than HCQ impact on controlled tissue or person. It means, HCQ effect on LQTS2 infected with *mild* COVID-19 does not show adverse effect as expected in control group treated with HCQ nor LQTS2 provided with HCQ. Even though in real scenario, HCQ is not provided for LQTS2 treatment, this finding would help in treating and managing LQTS2 infected with *mild* COVID-19

Under LQTS2 and *severe* COVID-19, the APD in mid cells decreases by 24%, higher than that of other cell types (14.3%). However, the decrease in plateau peak in mid cells is lower (8.42%) in comparison to other cell types (17.36%). The change in APD on adding HCQ is negligible while the peak plateau potential further decreases by 22.99% in all cells types with respect to control values. To be particular, HCQ treated for COVID-19 mid cell's APD increases by 1.28% and plateau peak decrease by 15.05%, which is very high comparing to endo and epi cell.

Thus, its evident that using HCQ for pre-existing LQTS patient would result in EADs in mid cells which are likely to act as a source of reentry for initiating or sustaining an arrhythmia, which is not in clinical practice. However, LQTS infected by COVID-19 and when treatment with HCQ, it does not induce EAD but prolongation of APD is observed in *mild* than *severe* COVID-19.

3.1.3 HCQ Effect on Cardiac Myocytes with Hypokalemia Conditions

Hypokalemia condition is further classified into mild, moderate and severe conditions based on the extracellular potassium concentration (K_o^+) by decreasing K_o^+ to 85% (hypokalemia1), 55%

(hypokalemia2) and 45% (hypokalemia3) respectively as shown in Fig. 1(xiii-xxi).

***Hypokalemia1 with COVID-19*:** In hypokalemia1, the resting potential (V_{rest}) decreases from -85.97 mV in control condition (in all three cells) to -88.26 mV, -89.16 mV and -88.55 mV in endo, mid and epi cells respectively. The percentage △APD between control and hypokalemia1 is higher in mid cells (2.35%) compared to endo (0.79%) and epi cells (0.98%) and △ plateau peak is about 0.9% in three cells respectively. On HCQ including with hypokalemia1, the △APD in endo, mid and epi cells is further increased from control values to 4.13%, 10.34% and 4.47% respectively. Further, V_{rest} decreases to -88.7 mV, -89.20 mV and -88.90 mV and the difference in plateau peak is 5.60%, 5.96% and 5.91% in endo, mid and epi cells respectively.

Comparing the control and combination of Hypokalemia1 and *mild* COVID-19, the APD in endo, mid and epi cells is decreased by 3.12%, 5.88% and 2.92% respectively. The peak plateau potential is reduced by an average of 4.89%. With HCQ, the APD reaches near-control values while the peak potential is reduced by an average of 9.84%. Under Hypokalemia1 and *severe* COVID-19, the APD in mid cells is decreased (30.56%) more than that of other cells (19.73%) and the peak potential decreases by an average of 19.06% in comparison to control. With HCQ, the APD is almost similar while the peak potential further reduces by 24.32%. Further, the endo, mid and epi cells get hyperpolarised to -89.46 mV, -89.78 mV and -89.57 mV respectively in the absence and presence of HCQ for both *mild* and *severe* COVID-19.

***Hypokalemia2 with COVID-19*:** Likewise, the percentage △APD between control and hypokalemia2 is 8.87% in mid cells compared to endo (3.79%) and epi (3.72%) cells, while the difference in plateau peak is an average of 3.18% in three cell types respectively. On including HCQ with hypokalemia2, the △APD in endo, mid and epi cells is further increased from control values to 8.55%, 21.30% and 8.52% respectively with a △plateau peak is 7.82%, 5.96% and 8.33% in endo, mid and epi cells respectively.

Comparing control with the combination of Hypokalemia2 and *mild* COVID-19, the change in APD in all cell types is minimal (less than 1%) while the peak plateau potential is reduced by an average of 6.92%. With HCQ, the APD increase in mid cells (6.33%) is higher than other cells (3.59%) in comparison to control while the peak potential is reduced by an average of 11.95%. In Hypokalemia2 and *severe* COVID-19, the reduction in APD in mid cells is higher (28.10%) than endo (18.07%) and epi (17.46%) cells and the peak potential decreases by an average of 20.49% in comparison to control. With HCQ, the reduction in APD is increased slightly in endo (16.68%), mid cells (26.48%) and epi (16.10%) cells while the peak potential further reduces by 25.85%. The resting potential of all cells is increased to -99. 87 mV, -100.44 mV and -99.65 mV in endo, mid and epi cells in absence and presence of HCQ for both *mild* and *severe* COVID-19.

***Hypokalemia3 with COVID-19*:** The percentage △APD between control and hypokalemia3 is 5.30%, 12.29% and 5.05% in endo, mid and epi cells respectively and the difference in plateau peak is about 4.15%. On including HCQ condition with hypokalemia3, the △APD in endo, mid and epi cells is further increased from control values to 10.84%, 27.52% and 10.66% respectively.

The difference in plateau peak is 8.73%, 9.41% and 9.35% in endo, mid and epi cells respectively.

In hypokalemia3 and *mild* COVID-19 condition, the APD is increased by 0.89%, 1.43% and 0.95% in endo, mid and epi cells respectively versus control. The peak plateau potential is reduced by an average of 7.80% in all cells. The APD on adding HCQ,is further increased to 9.88% in mid cells and 5.6% in endo and epi cells versus control while the peak plateau potential is reduced by an average of 12.84% in all cells.

Comparing control with hypokalemia3 and *severe* COVID-19, the decrease in APD in mid cells (26.91%) is higher than endo (17.00%) and epi (16.48%) cells. The decrease in peak plateau potential is an average of 21.07% in all cells. On adding HCQ, the reduction in APD is increased slightly in endo (15.27%), mid cells (25.21%) and epi (14.71%) cells while the peak potential further reduces by 26.45% in all cells. The resting potential of all cells is increased to -104.89 mV, -105.03 mV and -104.95 mV in endo, mid and epi cells in absence and presence of HCQ for both *mild* and *severe* COVID-19.

Result infers that the mid cells undergoing a more pronounced elongation making them vulnerable to EAD development in the case of LQTS. In LQTS2 with *mild* COVID-19, the mid cells have a higher APD prolongation than other cells. Uniquely, the increase in APD of mid cells in the case of LQTS1 with *mild* COVID-19 is lesser than other cells. The combination of LQTS1 or LQTS2 with *severe* COVID-19 causes a reduction in the APD in all cells without and with HCQ. The reduction in mid cells being more pronounced than that of endo and epi cells. The combination of hypokalemia and COVID-19 decreases the APD except in the case of hypokalemia 2 and *mild* COVID-19, hypokalemia 3 and *mild* COVID-19 and with HCQ. The mid cells undergoing a more pronounced effect than endo or epi cells. The plateau peak is decreased in all cases and the addition of HCQ enhances this effect. Further, hyperpolarization of the cells has been shown to induce arrhythmia via development of after depolarisations[40]. In addendum, HCQ treatment has the adverse effect of further prolonging the APD and thus acting as a causative agent for arrhythmia.

		Condition		Condition with HCQ	
	Cell Type	APD_{90}	Plateau Peak	APD_{90}	Plateau Peak
Control	Endo	277.63	35.15	285.62	33.50
	Mid/M	356.18	36.55	380.12	34.72
	Epi	271.76	36.35	279.74	34.54
Mild COVID-19	Endo	267.19	33.73	273.09	32.08
	Mid/M	328.72	35.04	344.73	33.02
	Epi	262.142	34.87	268.04	33.04
Severe COVID-19	Endo	220.30	28.79	221.195	27.11
	Mid/M	244.53	29.69	245.62	27.72
	Epi	217.67	29.76	218.36	27.64
LQTS1	Endo	320.29	35.31	334.39	33.65
	Mid/M	406.55	36.58	838.37	34.75
	Epi	313.57	36.48	326.61	34.66

LQTS1 and Mild COVID-19	Endo	302.19	33.87	312.63	32.
	Mid/M	357.95	33.85	383.44	33.22
	Epi	297.00	34.985	306.605	33.15
LQTS1 and Severe COVID-19	Endo	236.09	28.86	237.36	27.17
	Mid/M	252.13	29.7	252.46	27.74
	Epi	233.68	29.66	234.63	27.69
LQTS2	Endo	298.38	35.53	301.38	33.76
	Mid/M	446.87	36.95	657.97	35.00
	Epi	290.79	36.75	295.01	34.82
LQTS2 and Mild COVID-19	Endo	286.37	34.10	288.69	32.34
	Mid/M	380.24	35.43	389.51	30.05
	Epi	280.4	35.26	282.60	33.32
LQTS2 and Severe COVID-19	Endo	236.96	29.12	233.87	27.33
	Mid/M	268.73	33.47	264.17	27.97
	Epi	233.65	29.96	230.67	27.89
Hypokalemia1	Endo	279.84	34.84	289.10	33.18
	Mid/M	364.56	36.21	393.02	34.37
	Epi	274.43	36.01	283.91	34.19
Hypokalemia1 and Mild COVID-19	Endo	268.96	33.45	276.55	31.80
	Mid/M	335.22	34.73	353.39	32.88
	Epi	263.82	34.578	271.10	32.73
Hypokalemia1 and Severe COVID-19	Endo	221.84	28.60	223.43	26.91
	Mid/M	247.32	29.47	249.39	27.46
	Epi	219.09	29.37	220.49	27.39
Hypokalemia2	Endo	288.16	34.05	301.38	32.40
	Mid/M	387.77	35.37	432.06	33.49
	Epi	281.86	35.192	294.92	33.32
Hypokalemia2 and Mild COVID-19	Endo	276.44	32.76	287.56	31.11
	Mid/M	352.68	33.97	378.75	32.08
	Epi	270.86	33.82	281.59	31.93
Hypokalemia2 and Severe COVID-19	Endo	227.45	28.15	231.29	26.46
	Mid/M	256.06	28.92	260.83	26.87
	Epi	224.30	28.83	227.98	26.77
Hypokalemia3	Endo	292.36	33.73	307.74	32.08
	Mid/M	399.99	35.00	454.21	33.11

	Epi	285.49	34.83	300.73	32.95
Hypokalemia3 and Mild COVID-19	Endo	280.12	32.48	293.19	30.83
	Mid/M	361.28	33.64	391.38	31.74
	Epi	274.34	33.49	286.97	31.60
Hypokalemia3 and Severe COVID-19	Endo	230.26	27.98	235.23	26.29
	Mid/M	260.30	28.69	266.37	26.62
	Epi	226.96	28.6	231.76	26.53

Table 2: Action potential duration and Plateau peak metrics of all the three setups for various condition

3.2 Heterogeneous Cardiac Tissue Mechanism(s) in Control, COVID-19, and Comorbid Conditions

To understand the spatiotemporal mechanism of the cardiac tissue, a framework consisting of three layers (endo, mid and epi) of cardiomyocytes is developed and the lower leftmost corner (Cells 1:10,1:2) of the tissue is stimulated. As a result of this stimuli, a convex wavefront propagates from the endo to mid and epi layer from the bottom to the top of the tissue. The repolarisation occurs first in the epi and endo layers, and M-cells in the mid layer are the last to repolarise. Normalised pseudo ECGs are synthesized from this tissue. *Mild* and *severe* COVID-19 conditions are introduced in the tissue to study its effect without and with HCQ. Furthermore, other comorbidities such as LQTS1, LQTS2 and hypokalemia are included to understand the its influence on COVID-19 conditions. In each of these conditions, the QT interval and T-peak amplitudes are recorded in Table 3.

In control, the QT interval is observed to be 0.345 s and the T-peak occurs at 0.2265 mV. In presence of mild COVID-19, the QT interval is shortened by 5.79% (0.325) sec and T-peak decreases by 33.33% (0.151 mV) as seen in Fig. 2(i). In combination with HCQ drug, the QT interval slightly increases by 1.45% (0.340 sec) and T-peak rises by 20.08% (0.181 mV) in comparison with no HCQ. However, it doesn't reach the control values. Under severe COVID-19 conditions, the QT interval is further reduced by 20.29% (0.275 s) and a negative T-wave peak of -0.17 mV is observed along with a QT depression. This negative T-peak might be representative of ischemia in clinical ECG recordings[41]. In contrast, the effect of HCQ in *severe* COVID-19 is negligible with QT interval duration remaining the same and T-peak increasing slightly to -0.153 mV. Here we have considered a pacing interval of 800 msec (i.e HR is 75 beats/min), so the Bazett QT_c interval is 0.363 sec and 0.307 sec in *mild* and *severe* COVID-19 conditions. A study by Anttonen *et al.,*[42] reported that an individual's QT_c interval $<$320 msec is a low rate of all-cause mortality, from which we infer that a patient with *severe* COVID-19 is thus not at high risk of mortality from cardiac failure or disorder; unless and otherwise in presence of other comorbidities. On adding HCQ, the QT_c interval is in increased to 0.380 sec in *mild*, while it remains the same in *severe* COVID-19 conditions.

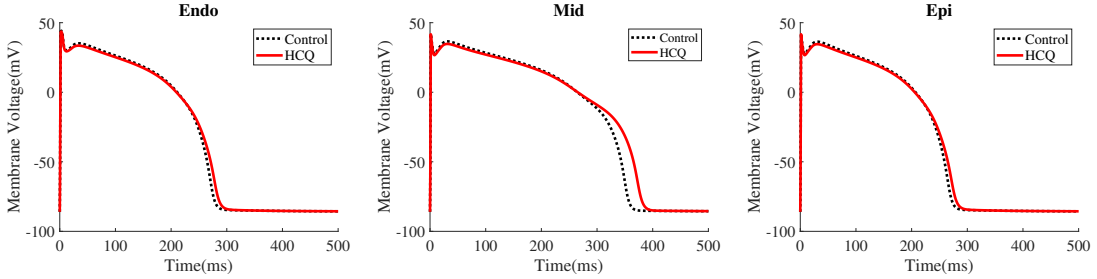

(i) (ii) (iii)

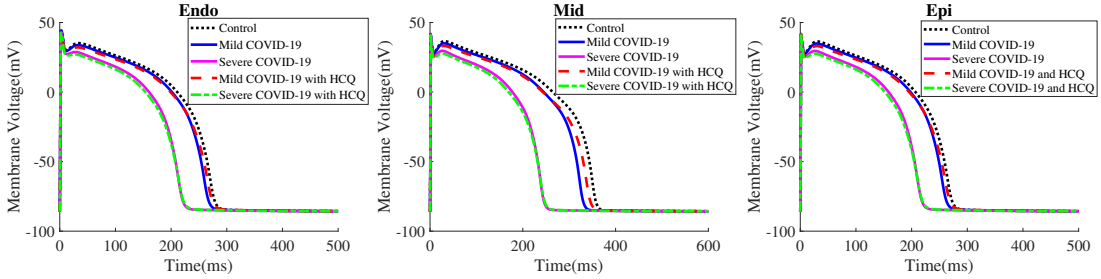

(iv) (v) (vi)

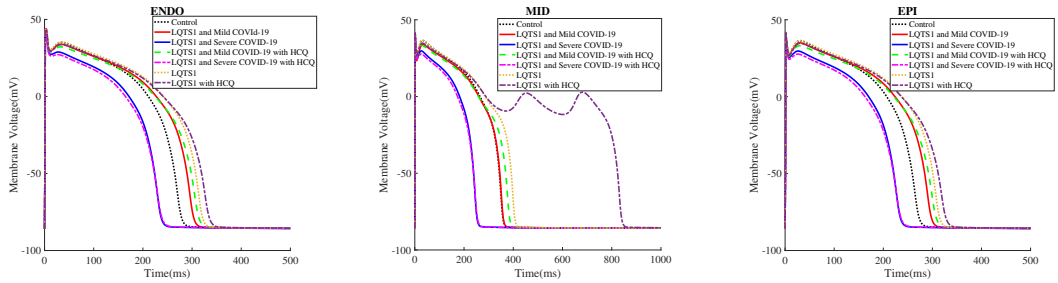

(vii) (viii) (ix)

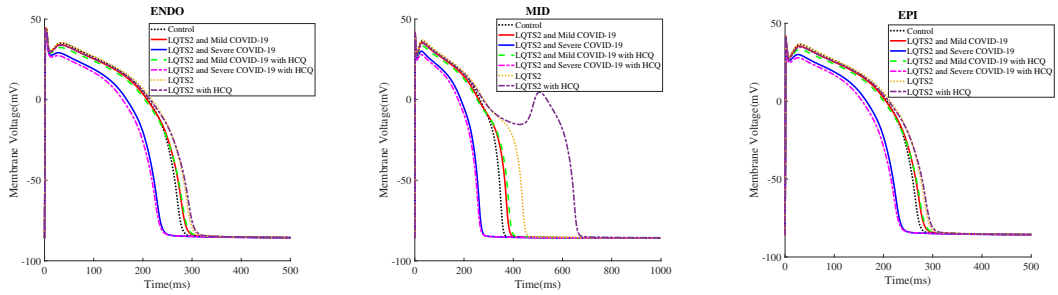

(x) (xi) (xii)

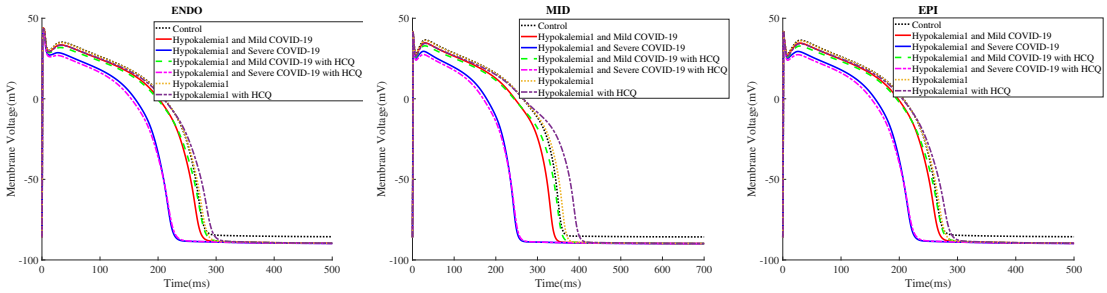

(xiii) (xiv) (xv)

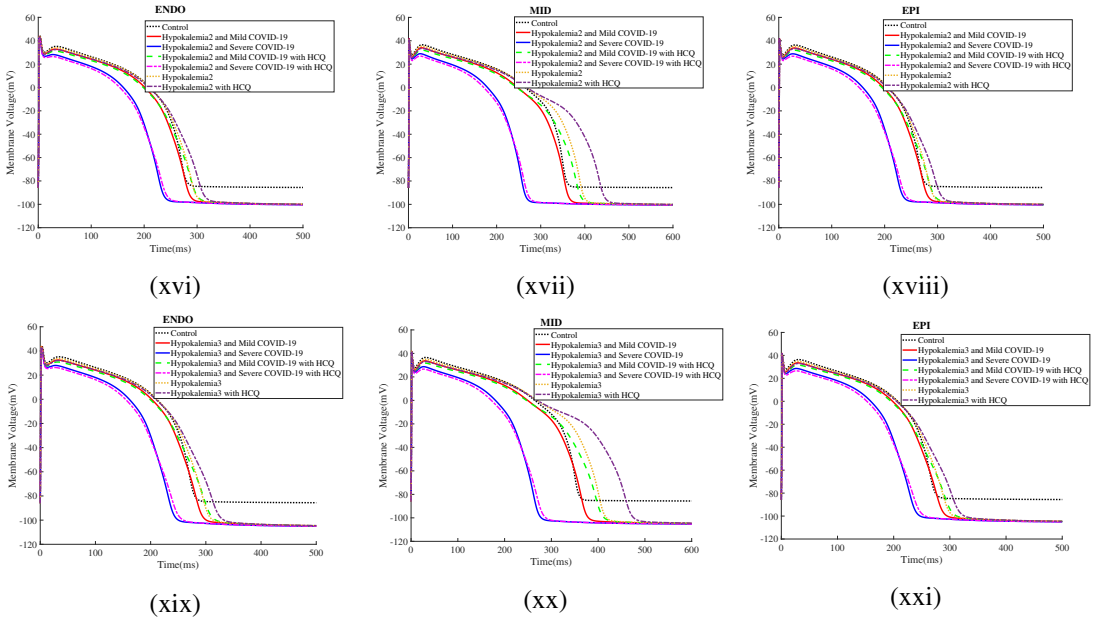

Figure 1: Cardiac ventricular action potential mechanism of cardiac myocyte cell such as Endo, Mid and Epi cells has been tested for various pathophysiological condition (i-iii) control myocyte cell treated with HCQ, (iv-vi) Mild and severe COVID-19 condition with HCQ drug effect, (vii-ix) pre-existing LQTS1 with HCQ, (x-xii) pre-existing LQTS2 treated with HCQ and (xiii-xv) Hypokalemia (three stages) with HCQ

Mercuro et al.[26] reported that in 90 COVID-19 patients, the median baseline QT_c was 455 (430-474) ms in control vs 473 [454-487] ms in HCQ conditions. The QT_c values reported in our study are lower than those observed clinically due to the limitation of considering only a segment of the ventricle. However, the percentage increase in APD between control and HCQ in the clinical study of Mercuro et al. is 3.95%. On comparing the percentage change in QT_c in *mild* COVID-19 and on including HCQ, an increase in 4.68% is observed.

On introducing LQTS1 and LQTS2 conditions with properties described in Table. 1, an increase in QT interval by 11.59% (0.385 s) is observed in each case as seen in Fig. 2(ii). However, the T-peak is reduced by 7.28% (0.210 mV) in LQTS1 while it is increased by 38.18% (0.313 mV) in LQTS2 condition. When treated with HCQ, the QT interval is further prolonged by 20.29% (0.415 sec) and 14.49% (0.395 sec) with increase of T-peak by 26.27% (0.286 mV) and 43.29% (0.326 mV) in LQTS1 and LQTS2 respectively. Further, in *mild* COVID-19 tissue with comorbid LQTS1 condition, QT interval increases by 7.24% (0.370 s) with a notched T-wave pattern of two peaks appearing at 0.1065 mV and 0.0961 mV as seen in Fig. 2(iii). Further, HCQ drug impacts the QT interval and T-peak by increasing them by 13.04% (0.390 s) and 30.24% (0.158 mV) respectively. Whereas, in *severe* COVID-19 with LQTS1, the QT interval is reduced by 14.49% (0.295 ms) and a negative T-peak amplitude of -0.262 mV is observed. The QT interval remaines the same in presence of HCQ while the T-peak only slightly increases to -0.238 mV. This inverted T-wave morphology could be due to bundle block, hypertrophy effect or pulmonary embolism[41].

Similarly, in the case of LQTS2 and *mild* COVID-19, the QT interval and maximum T-peak increases by 8.69% (0.375 sec) and 8.16% (0.245 mV) respectively (as seen in Fig. 2(iv)). On

introducing HCQ, there is no change in the QT interval while T-peak raises by 11.25% (0.252 mV) in comparison to control. In *severe* COVID-19 and LQTS2, the QT interval is the same 0.300 mV and a biphasic T-wave of amplitude 0.015 mV and -0.075 mV (without HCQ) is found despite of HCQ addition.

Thus, this study infers that when an individual with pre-existing LQTS condition gets infected by *mild* COVID-19, a prolongation of the QT interval occurs and the inclusion of HCQ adds further to the extension of QT interval. The finding of inverted T-wave in LQTS1 or LQTS2 and *severe* COVID-19 is suggestive of an ischemic pattern. This could be one of the reasons that explains why COVID-19 patients with comorbidities are at a higher risk of mortality. Furthermore, the presence of HCQ does not create any alterations in the pseudo ECG pattern. An inverted T-wave pathology could be indicative of an ischemia or hypokalemia condition, this demands us to investigate and understand the mechanism of hypokalaemia in COVID condition in the next section.

Fig. 2(v-viii) shows the pseudo ECGs generated for the different combinations of Hypokalemia and COVID-19 as well as in presence of HCQ. In comorbid hypokalemia1 condition as seen in Fig. 2(v), the QT interval increases by 2.89% (0.355 sec), while the peak amplitude of T-wave increases only by 1.10% (0.229 mV), almost similar to control condition. When exposed to HCQ, the QT interval increases by 8.69% (0.375 msec) and T-peak amplitude increases by 16.99% (0.265 mV) in comparison to control. But, when infected by *mild* COVID-19, the QT interval decreases by 2.89% (0.335 sec), yet a notched T-wave appears with the first T-peak of 0.127 mV and second peak of 0.153 mV is observed. On adding HCQ, the notched T-wave are replaced by positive T-waves. The QT interval is increased by 1.45% (0.350 mV) and T-peak is reduced by 17.88% (0.186 mV) in comparison with control. In contrary, in pre-existing hypokalemia1 conditions infected severely with COVID-19, the QT interval reduces by 17.39% (0.285 s) and a negative T-peak of 0.16 mV is observed in comparison with control (i.e suggestive of ischemia disorder). HCQ drug does not have any noteworthy effect other than slight reduction of T-peak to -0.14 mV.

In hypokalemia2, the QT interval is prolonged further by 10.14% (0.380 ms) but a reduction in T-peak by 4.19% (0.217 mV) is observed. HCQ exposure increases QT interval by 18.84% (0.410 ms) with 12.58% (0.255 mV) increase in T-peak. On considering hypokalemia2 and *mild* COVID-19, the QT interval increases by 2.89% (0.355 s) while T-peak reduces by 37.74% (0.141 mV) in comparison to control. On including HCQ, the QT interval is prolonged by 10.14% (0.380 sec) and the T-peak is reduced by 23.17% (0.174 mV). Similar to hypokalemia1 infected COVID-19 scenario, in hypokalemia2 and *severe* COVID-19, a negative T-peak of 0.156 mV is observed with reduced QT interval of 13.04% (0.300 sec). Here too, HCQ has no significant effect, other than a slight increase in the QT interval and T-peak to 0.305 s and 0.126 mV respectively.

Finally, in hypokalemia3, the QT interval is prolonged further by 13.04% (0.390 msec) while the T-peak is reduced by 7.28% (0.210 mV), similar to that seen in presence of hypokalemia2. In presence of HCQ, the QT interval increases by 23.18% (0.425 msec) and the T-peak increases by 8.61% (0.246 mV) with respect to control. *Mild* COVID-19 infection has the effect of increasing the QT interval by 5.79% (0.365 sec) and reducing the T-peak by 41.28% (0.133 mV). HCQ treatment further prolongs the QT interval by 14.49% (0.395 sec) and the T-peak reduces by 25.82% (0.168 mV). During *severe* COVID-19 with hypokalemia3 also, a negative T-peak of

-0.155 mV with 10.14% reduction of QT interval (0.310 sec) is observed. In hypokalemia3 and *severe* COVID-19 condition, the QT interval is reduced by 10.14% (0.310 sec) and a negative T-peak of -0.155 mV is observed. On adding HCQ with the above conditions, the QT interval increases to 0.320 s and the T-peak becomes slightly less negative at 0.121 mV.

Thus, it can be summarized that irrespective of the severity level of a preexisting hypokalemic condition, getting severely infected by COVID-19 can proliferate the risk factor due to the presence of inverted T-wave, that implies the occurrence of ischemia. Even though the scope of this study is limited to cardiac diseases or variabilities in cardiac system, hypokalemia can be trigged due to imbalance electrolyte imbalance or if they are the manifestation of renal diseases[?] . Thus its unclear about *severe* COVID-19 is whether the T-wave inversion is associated with cardiac complications or renal disorder cause electrolyte imbalance.

3.3 Arrhythmogenesis Effect of HCQ on COVID-19 Infected Tissue - without and with Comorbidities

3.3.1 Premature pacing sequence protocol

Scientific community had well accepted that, early or late phase of replarization of the ventricular AP are the manifestation of ion imbalance and controlled by different mechanistic; this are involved in or responsible for various life-threatening cardiac disease. To analyze arrhythmia occurrence, the cardiac tissue is paced with premature beats (PBs) in presence of the normal pacing beats of 800 ms (75 bpm). It has been reported[43] that QT_c formulae will lead to false negative diagnosis at higher heart rate, so QT interval measured is accurate at heart rate $<$100bpm, further it has been recommended as $<$80 bpm. Here, three consecutive PBs as shown in Fig. 3 (single or two PBs are not effective in creating an arrhythmia) are applied, to strive in initiating an arrhythmic pattern. The duration of PBs in each case is determined by the time the endo cells located at the bottom of the tissue have come out of their refractory state and are re-excitable again. Initially, the presence of PBs in *mild* and *severe* COVID-19 configurations are tested to examine if an arrhythmia occurs. Next, other comorbidities mentioned in Section 2.1: LQTS1, LQTS2 and hypokalemia are included to understand which conditions give rise to an arrhythmia. Finally, the comorbidities along with COVID-19 infection are tested by the same pacing protocol. In each condition, the inclusion of HCQ is also examined.

3.3.2 Cardiac Tissue Arrhythmogenesis Response in Presence of COVID-19 Infection and its Effect for HCQ

Fig. 4 shows the pseudo ECG on including *mild* and *severe* COVID-19 conditions in the tissue and on HCQ exposure. Under *mild* COVID-19, three PBs each of 295 msec duration are applied after the first beat. The mid cells in the tissue are in a repolarising state when the first PB is applied. This causes the depolarisation from the first PB to travel upward along the endo layer and later depolarize the mid and epi layer. Repolarisation occurs from the endo, mid and then epi layer which appears as a negative T-wave in the ECG in Fig. 4(i). The depolarisation wavefront from the second PB is not able to excite the cells in the epi layer as they are in a refractory state and

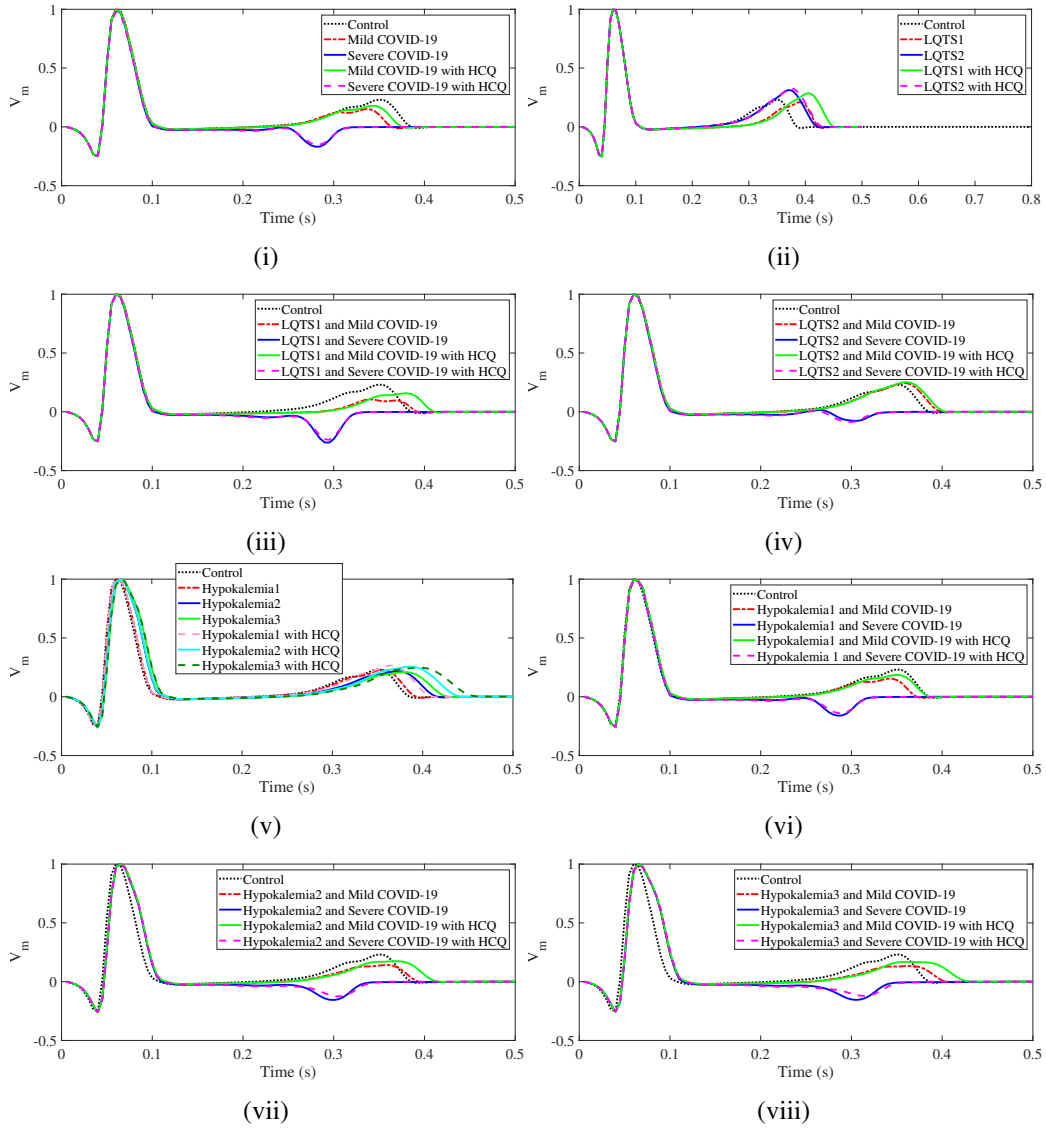

Figure 2: Pseudo ECGs generated in control and in presence of HCQ under (i)*mild* and Severe COVID-19 (ii) LQTS1 and LQTS2, (iii) LQTS1 and COVID-19, (iv)LQTS2 and COVID-19, (v)Hypokalemia, (vi)Hypokalemia1 and COVID-19, (vii)Hypokalemia2 and COVID-19 and (viii)Hypokalemia3 and COVID-19

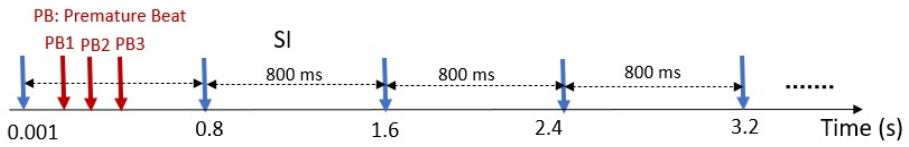

Figure 3: Premature Pacing Protocol: Three premature beats are applied after the first normal pacing pulse. Regular pacing duration is 800 ms.

this appears as a ST segment elevation. Further, when the third PB occurs, an inverted T-wave is created as the mid and epi cells repolarise simultaneously. Later, normal pacing pulses are resumed at 1.6 sec in both the cases. Presence of HCQ shows a similar trend. Our study is in line

with those reported by Wang et al.,[20] where a dosage of 10 μM HCQ prolonged the APD of cells but didn't induce an arrhythmia in tissue on decreasing the pacing interval.

In *severe* COVID-19, the three PBs are applied every 250 msec. The application of three PBs leads to an ECG pattern with an increase in the negative amplitude of the T-peak due to the changes in depolarisation and repolarisation pattern same as that of the first PB in mild COVID-19 case. The first and third PBs create ECGs with an increased amplitude of negative T-peak compared to that created by the second PB. The normal ECGs are resumed at 1.6 sec in both scenarios. Thus, it can be inferred that an inverted T-wave morphology (representative of ischemia) can be used as a bio-marker for *severe* COVID-19 conditions. Further, HCQ drug causes negligible modifications in the voltage propagation patterns and no effect has been observed in the ECG compared with control.

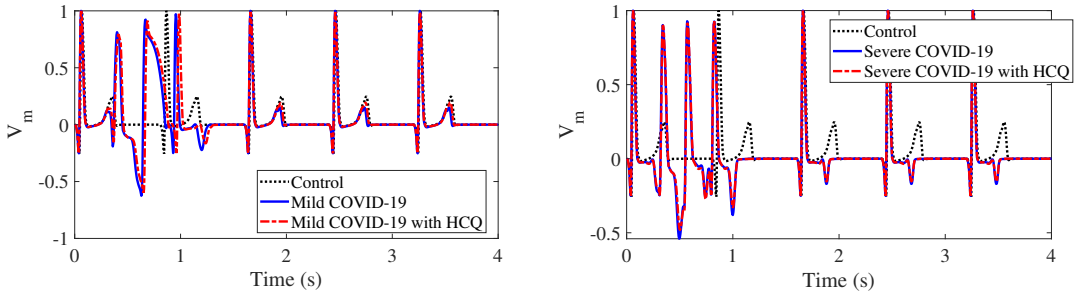

(i) (ii)

Figure 4: Pseudo ECG for i)Mild COVID-19 and HCQ ii)Severe COVID-19 and HCQ

3.3.3 Cardiac Tissue Arrhythmogenesis Response in Pre-existing Long QT Syndrome Infected by COVID-19 and Effect of HCQ Drug

***LQTS1 and COVID-19*:** LQTS1 conditions are introduced in the cardiomyocytes and after the first pacing pulse, three premature beats each of 350 ms duration are applied at the same pacing site and the pseudo ECG is recorded as indicated in Fig. 5(i). The first PB is applied when the mid cells are in refractory state, hence the depolarisation wavefront travels upwards along the endo layer and then proceeds into the mid and epi layers. Thus, the repolarisation pattern changes with the mid cells repolarising before the epi cells thereby giving rise to an inverted T-wave. It is observed that the second PB creates an elevated ST segment, this is because the cells in the epi layer don't get depolarised as they are in refractory state due to the application of the first PB. The third PB gives rise to a biphasic T-wave of 0.055 mV and -0.132 mV due to the delayed repolarisation of epi cells. On adding HCQ and pacing with PBs of 360 ms, the first PB creates a pattern similar to that observed without HCQ. However, the application of second PB depolarises the epi cells also and a negative T-wave is observed in Fig. 5(i). The third PB depolarises all the cells also. These changes in the depolarisation and repolarisation pattern gives rise to the pseudo ECG waveform, however no reentry is generated and the normal propagation pattern is resumed at 1.6 sec in both the scenarios. Further, when LQTS1 is exposed to COVID-19 there response during PBs are captured by generating a pseudo ECGs as shown Fig. 5(ii).

In case of LQTS1 and *mild* COVID-19 conditions, PBs are applied every 330 ms and the first and third PB gives rise to inverted T-waves while the second PB creates an upright T-wave. On including HCQ, and pacing the tissue with PBs each of 355 ms, a similar pattern of pseudo ECG is obtained although with an extension of the QT interval. Under LQTS1 and *severe* COVID-19 conditions, three PBs each of 265 ms, are applied and this creates the pseudo ECG pattern seen in Fig. 5(iii). The first and third PBs create ECGs with an increased amplitude of negative T-peak compared to that created by the second PB. A similar ECG pattern is found on including HCQ. In all the above scenarios, the normal pulses are resumed after a long pause at 1.6 sec.

***LQTS2 and COVID-19*:** In the case of LQTS2, PBs are applied every 330 ms and 340 ms without or with HCQ respectively. When the first PB is applied , the mid cells are in repolarising state and hence the depolarisation wavefront travels along the endo layer and later moves into the mid and epi layer. This same pattern is repeated for the next two PBs and thus no reentry of wave propagation occurs. These changes in the depolarisation and repolarisation creates the pseudo ECG pattern in Fig. 5 (iv) and HCQ has no effect as it follows a similar trend.

Fig. 5(v-vi) compares the pseudo ECGs generated on pacing the tissue with PBs, each of 315 ms and 265 ms, in LQTS2 and *mild* COVID-19 conditions versus LQTS2 and *severe* COVID-19 conditions respectively. In both cases, the PBs generate negative T-waves although the QRS complexes obtained in *mild* COVID-19 are wider. No arrhythmic pattern is generated and the regular pacing pattern of 800 ms is resumed from from 1.6 s. ECGs in severe COVID-19 are observed to create biphasic T-waves. On including HCQ and pacing the tissue with PBs, a similar pattern of pseudo ECG is obtained in both *mild* and *severe* COVID-19, although with an extension of the QT interval.

The net result of this study infers that the inverted T-wave morphology seen in all *severe* COVID-19 conditions and the notched T-waves morphology observed in LQTS 1 & *mild* COVID-19 conditions, clinically represent preponderant right or left ventricular hypertrophy and bundle branch block, which is out-of-scope of this study and it requires further investigation.

3.3.4 Cardiac Tissue Arrhythmogenesis Mechanism in Presence of Pre-existing Hypokalemia and COVID-19 and When Treated with HCQ

To investigate the impact of COVID-19, pseudo ECGs are generated on pacing the tissue with PBs in the presence of different degree of Hypokalemia, severity of COVID-19 and on including HCQ.Fig. 6 shows the pseudo ECGs generated after pacing the tissue with PBs for the above mentioned conditions.

***Hypokalemia1 infected with mild COVID-19, with and without HCQ*:**The tissue is regularly paced every 800 msec. After the first pacing pulse, three premature beats each of 305 msec duration are applied at the same pacing site as indicated in Fig. 6(i). It is observed that in the case of hypokalemia1, reentrant activity is generated from 0.37 sec to 1.39 sec and normal beats are resumed from 1.6 sec. On including HCQ and applying three PBs at 325 msec duration each,

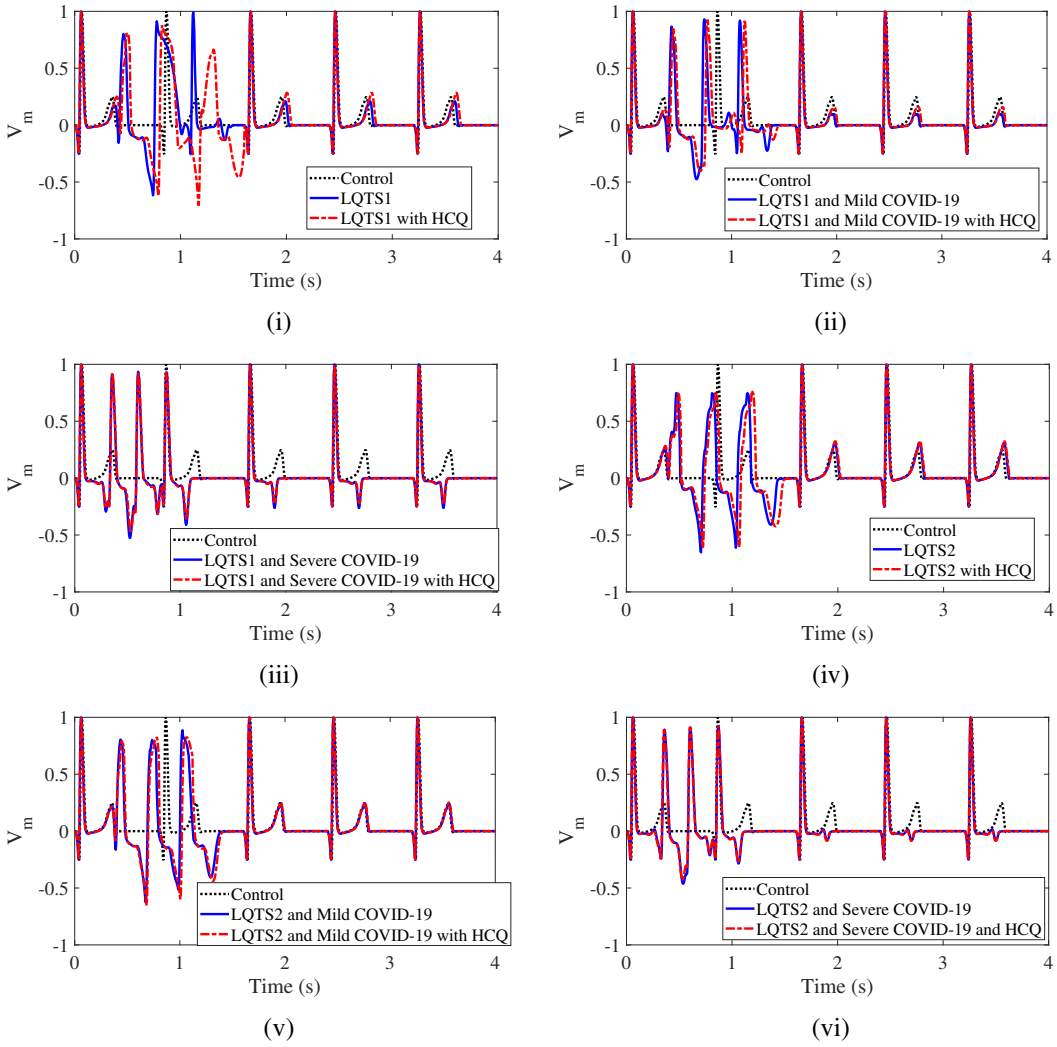

Figure 5: Comparison of Pseudo ECGs for i)LQTS1 and LQTS1 with HCQ, ii)LQTS1 and Mild COVID-19 with HCQ iii)LQTS1 and severe COVID-19 with HCQ iv)LQTS2 and LQTS2 with HCQ, v)LQTS2 and Mild COVID-19 with HCQ vi)LQTS2 and Severe COVID-19 with HCQ

reentrant activity is generated from 0.38 sec to 2.2 sec and it resumes to normal from 2.4 sec. Hence, there is a 43.96% risk in the arrhythmic activity.

In Fig. 6(ii), hypokalemia1 and *mild* COVID-19 conditions are included in the tissue, three PBs each of 295 msec are applied after the first beat. The regular pacing interval is 800 ms. When the tissue is excited due to the first PB, the cells in top of endo layer and those in mid and epi layers are in repolarising state. Thus, the wavefront from first PB travels upwards along the endo layer and propagates into the mid and epi layer. When the second PB occurs at 0.59 sec, the mid and epi cells are in repolarising state, thus the wavefront propagates along the endo layer and then enters into the mid and epi layer from the bottom once they come out of refractory state. A similar excitation pattern is observed after the third PB is applied. These changes in depolarisation and repolarisation appears as an arrhythmic-like activity from 0.355 sec to 1.24 sec in the pseudo ECG and normal beats are resumed from 1.6 s. Therefore, it is to be noted that the reentrant activity is

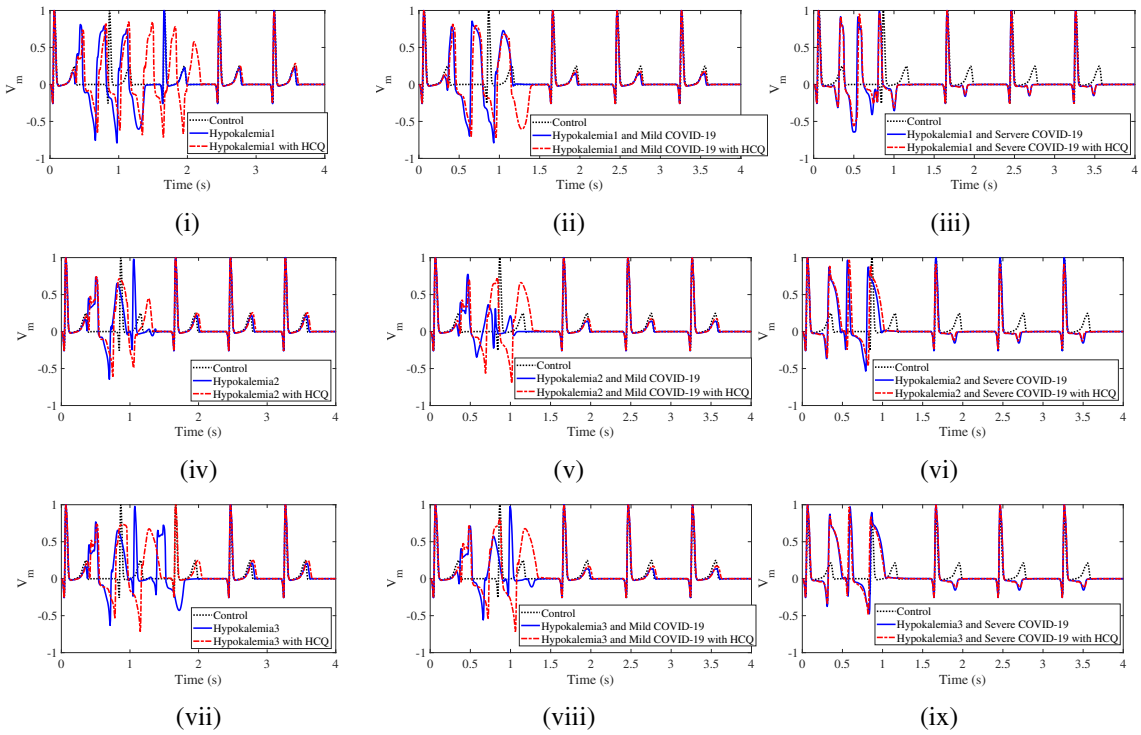

Figure 6: Pseudo ECG for i)Hypokalemia1 and treated with HCQ, ii)Hypokalemia1 with *mild* COVID-19 and treated with HCQ iii)Hypokalemia1 with *severe* COVID-19 and treated with HCQ ii) iv)Hypokalemia2 and treated with HCQ with HCQ, v)Hypokalemia2 with *mild* COVID-19 and treated with HCQ vi)Hypokalemia2 with *severe* COVID-19 and treated with HCQ, vii)Hypokalemia3 and treated with HCQ, viii)Hypokalemia3 with *mild* COVID-19 and treated with HCQ ix)Hypokalemia3 with *severe* COVID-19 and treated with HCQ

not generated in the voltage maps. The voltage maps are provided in Supplement 2. On including HCQ at 305 msec duration of three premature beats, a similar type of waveform is generated from 0.365 sec to 1.395 sec and normal beats are resumed from 2.4 sec. On the other hand, hypokalemia1 infected with *severe* COVID-19, the absence of HCQ creates a reentrant pattern from 0.315 s to 1.045 s on pacing the tissue with 3 PBs each of 250 ms duration as seen in Fig. 6(iii). On including HCQ and applying the same pacing protocol, reentry is not generated in the tissue. However, the excitation by the PB creates a similar appearance of ECG waveform. This difference can be seen in Fig. 6(iii) and the voltage maps are further illustrated in Supplementary-2. This shows that HCQ plays a vital role in pre-exisitng hypokalemia1 with COVID-19 cases.

***Hypokalemia2 infected with mild COVID-19, with and without HCQ*:** Applying three PBs each of 330 msec duration in between the normal pacing pulses in presence of hypokalemia2 doesn't generate any re-entrant activity as seen in Fig. 6(iv). The third PB at 0.99 sec generates a negative T-peak of 0.056 mV and the normal activity is resumed from 1.6 sec. However, in presence of HCQ with 355 msec PBs, reentrant activity is generated from 0.4 sec to 1.34 sec and the regular pacing sequence is resumed at 1.6 sec.

Hypokalemia2 and *mild* COVID-19 conditions are included in the tissue and paced with PBs

as shown in Fig.6(v). Reentrant activity is observed in the pseudo ECG after pacing with three PBs each of 300 msec duration from 0.355 sec to 0.935 sec.

In order to understand the detailed arrhythmogenesis mechanism in hypokalemia2 with *mild* COVID-19 conditions, voltage maps of cardiac tissue are shown in Fig. 7 starting from the application of the first PB at 0.300 sec. At this time, the endo cells at the top and the M-cells and epi cells are still in repolaring state. The depolarisation wave created from this first PB is shown in Fig. 7(a) at 0.31 sec. This wave proceeds upwards along the endo layer by which time the M-cells are returning to rest state as seen in Fig. 7(b). The wavefront then travels along the entire length of endo layer and reenters the mid and epi layers as seen in Figs. 7(c-d). This wavefront then reenters into the endo layer at the bottom of the tissue and travels upwards along the endo layer as seen in Fig. 7(e-f). The second PB is applied at 0.6 sec and during this time the endo cells are already depolarised. This wavefront re-enters into the mid and epi layers by which time the mid and epi cells have repolarised as seen in Fig. 7(g-i). The wavefront depolarises cells in mid and epi layers and reenters endo layer as seen in Figs. 7(j-k). The third PB is applied at 0.9 sec and the cells at the pacing site are already depolarised. The cells start repolarising from the epi, mid and endo with cells at the bottom of the endo and mid layer repolarising last as seen in Figs. 7(ii)(l-n). All the cells finally repolarise at 1.085 sec.

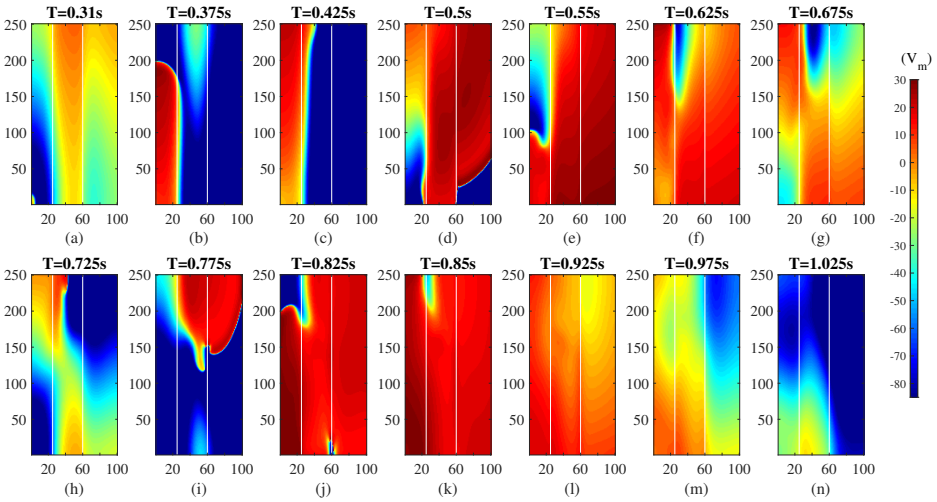

Figure 7: Voltage maps on applying PBs in Hypokalemia2 with Mild COVID-19

On adding HCQ and pacing the tissue with 3 PBs, each of 330 msec duration, in between the regular pacing interval of 800 msec, although arrhythmic-like activity is observed from 0.37 sec to 1.295 sec in the pseudo ECG, this is due to the depolarisation and repolarisation sequence of the cells in the tissue and not because of reentry which has been inferred form voltage map provided in Supplementary 1. Normal beats are resumed from 1.6 sec.

In case of *severe* COVID-19 conditions, the application of three PBs each of 250 msec, gives rise to the pseudo ECG shown in Fig.6(vi). The excitation of the first and third PB appear representative of an ST-elevation. On introducing HCQ, a similar ECG waveform is observed and no reentry of wavefront is observed.

***Hypokalemia3 infected with mild COVID-19, with and without HCQ*:** Similarly, in case of hypokalemia3, reentrant activity is not generated when pacing the tissue with 335 msec duration PBs as seen in Fig. 6(vii). Inclusion of HCQ casuses reentrant activity to appear from 0.415 sec to 1.45 sec on pacing with PBs of 355 msec duration. The regular pacing sequence is resumed at 1.6 sec. Even though HCQ drug is not intended for hypokalemia treatment, here we attempted to understand the role of HCQ in hypokalemia. Result infers that the presence of HCQ is pro-arrhythmic under all severity levels of hypokalemic and would have to be used with caution in such scenarios.

Fig.6(viii) shows the pseudo ECG on including Hypokalemia3 and *mild* COVID-19 conditions in the tissue and pacing with PBs. No reentrant activity is observed even after pacing with three PBs each of 310 msec duration. Similarly, on adding HCQ and pacing the tissue with 3 PBs, each of 330 msec duration, in between the regular pacing interval of 800 ms, no reentrant activity is generated.Normal beats are resumed from 1.6 sec. Under hypokalemia3 and *severe* COVID-19 conditions, the application of three PBs each of 265 ms, gives rise to the pseudo ECG shown in Fig.6(ix). Similar to earlier case of hypokalemia2 and severe COVID-19, the excitation of the first and third PB appear representative of an ST-elevation as the epi cells are not depolarised. Voltage maps of hypokalemia3 and *severe* COVID-19 conditions are shown in Fig. 8 provides insight on this observed response. The depolarisation wavefront created due to the first PB applied at 0.265 sec is seen in Fig. 8(a) and at 0.31 s, the mid and epi cells in the upper half of the tissue are still in repolarising state. This change in the repolarisation pattern (epi cells repolarising at the same time as mid cells) causes an inverted T-wave to appear in the pseudo ECG. The depolarisation wave from the first PB travels along the endo and mid layers (Fig. 8(b)). However, this wavefront doesn't enter the epi layer as they are in repolarising state. Thus, the endo and mid cells start repolarising as seen in Figs. 8(c-d), this gives rise to the raised ST-segment that appears in the pseudo ECG in Fig. 6(ix). The depolarisation wavefront from the second PB is observed in Figs. 8(e-g), travelling from endo to mid and epi layer. However, the repolarisation occurs in the endo layer followed by the mid and epi layer as seen in Figs. 8(h-i) which results in an inverted T-wave. When the third PB is applied at 0.795 s, the cells in the top of the mid and epi layer are still repolarising which causes the activation wavefront from the third PB to excite only the cells in endo and half of the mid layer as seen in Figs. 8(j-n). All the cells finally return to rest state at 1.04 sec. In this scenario treatment with HCQ creates a negligible difference in the pseudo ECG waveform.

Here, a 2D anisotropic transmural ventricular model is considered in which the entire mid layer is composed of M-cells with longer APD. However, certain studies have disputed the presence of M-cells[44,45] and others have debated that they form islands in the endo-mid interface[46,47]. Here, a premature pacing sequence is used to trigger an arrhythmic pattern. Other studies have reported the use of cross-pacing protocol[32] to simulate an arrhythmia in such in-silico models. This pacing sequence is not used here, as the propagation pattern would then travel parallelly along the entire length of the ventricle from endo, mid and epi and it would not mimic the actual depolarisation pattern in ventricle. Thereby, the generated pseudo ECG would appear irregular. Short-long-short (SLS) pacing sequences which are commonly observed to initiate a TdP pattern[48] is another

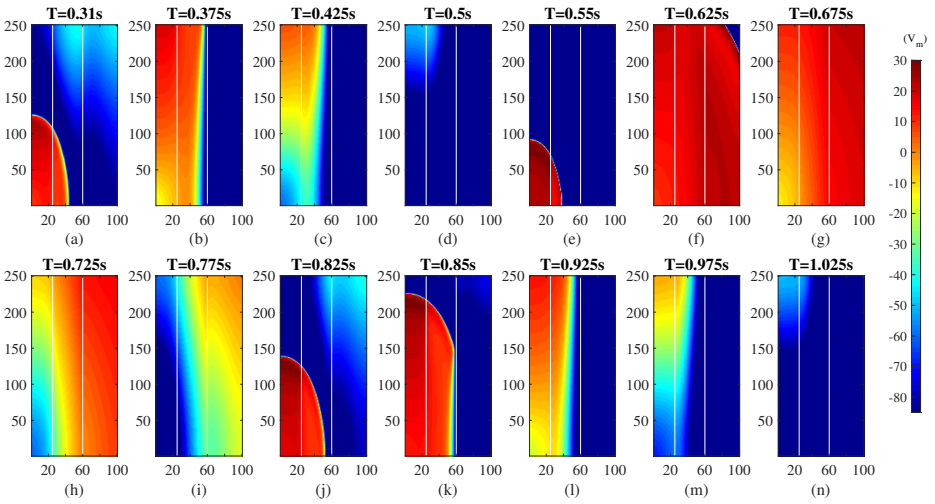

Figure 8: Voltage Maps on applying PBs in Hypokalemia3 and *Severe* COVID-19 with HCQ

option which would be tested in the future for the above scenarios. In clinical ECG recordings, self-terminating reentrant arrhythmia of few cycles may not be considered as critical. However, the limited duration of the reentry generated here is due to the consideration of the 2D ventricle model. In a three-dimensional or whole heart model, sustainable ventricular arrhythmias may occur. Based on the clinical study of [12], the effect of HCQ on the ionic currents of atrial myocytes for a specific dosage is adopted into this study of ventricular myocytes. The actual percentage variation in ionic currents based on the dosage of HCQ needs to be determined from in-vitro studies.

4 Conclusions

In this study, we present the first complete electrophysiological mechanism of COVID-19 with and without comorbidities such as Long QT syndrome and hypokalemia on the human ventricular myocytes and tissue and its responses to HCQ treatment. This model strategically allows more direct studies of ion channel perturbation from clinical observation of COVID-19 victims. The main conclusion of this study is, when healthy cardiac tissue is infected, it engenders shorter QT interval, low amplitude or inverted T-waves and ST depression; which could be used as biomarkers. When treated with HCQ, in case of *severe* COVID, there is no significant adverse effect, but in mild COVID-19, QT interval prolongs and T-peak increases in ECG. Secondly, COVID-19 infection withal to comorbid cardiac ventricle, causes a slight QT interval elongation, notched T-waves in mild COVID with LQTS1 or hypokalemia1, inverted T-waves in presence of all *severe* COVID-19 except in LQTS2 where biphasic T-waves are observed. In particular, the hypokalemic ventricle is prone to arrhythmia than long QT syndrome, when infected with COVID-19. However, in all hypokalemic conditions, HCQ drug has no significant effects on cardiac ventricle. Thus, the finding of in-silico models could be considered for management of COVID-19 patients with pre-existing pathologies.

Acknowledgements

We are grateful for the technical support of Rupam Chaudhury, Joshin S and Dr. Sundeep Khandelwal for their support in this project.

Conflict of Interest

None declared

References

1 Alhazzani W, Møller MH, Arabi YM, Loeb M, Gong MN, Fan E, et al. Surviving Sepsis Campaign: guidelines on the management of critically ill adults with Coronavirus Disease 2019 (COVID-19). Intensive care medicine. 2020;p. 1–34.

2 Madjid M, Safavi-Naeini P, Solomon SD, Vardeny O. Potential effects of coronaviruses on the cardiovascular system: a review. JAMA cardiology. 2020;.

3 Hosseiny M, Kooraki S, Gholamrezanezhad A, Reddy S, Myers L. Radiology perspective of coronavirus disease 2019 (COVID-19): lessons from severe acute respiratory syndrome and Middle East respiratory syndrome. American Journal of Roentgenology. 2020;214(5):1078–1082.

4 Shan F, Gao Y, Wang J, Shi W, Shi N, Han M, et al. Lung infection quantification of covid-19 in ct images with deep learning. arXiv preprint arXiv:200304655. 2020;.

5 James M Sanders TZJ Marguerite L Monogue, Cutrell JB. Pharmacologic Treatments for Coronavirus Disease 2019 (COVID-19): A Review. JAMA. April 13, 2020;p. E1–E13.

6 Sapp JL, Alqarawi W, MacIntyre CJ, Tadros R, Steinberg C, Roberts JD, et al. Guidance On Minimizing Risk of Drug-Induced Ventricular Arrhythmia During Treatment of COVID-19: A Statement from the Canadian Heart Rhythm Society. Canadian Journal of Cardiology. 2020;.

7 Yao X, Ye F, Zhang M, Cui C, Huang B, Niu P, et al. In vitro antiviral activity and projection of optimized dosing design of hydroxychloroquine for the treatment of severe acute respiratory syndrome coronavirus 2 (SARS-CoV-2). Clinical Infectious Diseases. 2020;.

8 Chen CY, Wang FL, Lin CC. Chronic hydroxychloroquine use associated with QT prolongation and refractory ventricular arrhythmia. Clinical Toxicology. 2006;44(2):173–175.

9 Nord JE, Shah PK, Rinaldi RZ, Weisman MH. Hydroxychloroquine cardiotoxicity in systemic lupus erythematosus: a report of 2 cases and review of the literature. In: Seminars in arthritis and rheumatism. vol. 33. Elsevier; 2004. p. 336–351.

10 Dan Zhou SMD, Tong Q. COVID-19: a recommendation to examine the effect of hydroxychloroquine in preventing infection and progression. Journal of Antimicrobial Chemotherapy. 11 May 2020;.

11 Andrea Savarino ACGM Johan R Boelaert, Cauda R. Effects of chloroquine on viral infections: an old drug against today's diseases. Lancet Infection Diseases. 2003;3:722–27.

12 Capel RA, Herring N, Kalla M, Yavari A, Mirams GR, Douglas G, et al. Hydroxychloroquine reduces heart rate by modulating the hyperpolarization-activated current If: Novel electrophysiological insights and therapeutic potential. Heart rhythm. 2015;12(10):2186–2194.

13 Rodriguez B. Multiscale modelling and simulation investigation of variability and abnormalities in repolarization: Application to drug cardiotoxicity. In: 2010 Computing in Cardiology. IEEE; 2010. p. 257–260.

14 Gautret P, Lagier JC, Parola P, Meddeb L, Mailhe M, Doudier B, et al. Hydroxychloroquine and azithromycin as a treatment of COVID-19: results of an open-label non-randomized clinical trial. International journal of antimicrobial agents. 2020;p. 105949.

15 Wang G, Tian X, Lu CJ, Flores H, Maj P, Zhang K, et al. Mechanistic insights into ventricular arrhythmogenesis of hydroxychloroquine and azithromycin for the treatment of COVID-19. bioRxiv. 2020;.

16 Ray WA, Murray KT, Hall K, Arbogast PG, Stein CM. Azithromycin and the risk of cardiovascular death. New England Journal of Medicine. 2012;366(20):1881–1890.

17 Amrita X Sarkar DJC, Sobie EA. Exploiting mathematical models to illuminate electrophysiological variability between individuals. The Journal of Physiology;590.

18 Burke RM. Active monitoring of persons exposed to patients with confirmed COVID-19—United States, January–February 2020. MMWR Morbidity and mortality weekly report. 2020;69.

19 Novel CPERE, et al. The epidemiological characteristics of an outbreak of 2019 novel coronavirus diseases (COVID-19) in China. Zhonghua liu xing bing xue za zhi Zhonghua liuxingbingxue zazhi. 2020;41(2):145–151.

20 Wang D, Hu B, Hu C, Zhu F, Liu X, Zhang J, et al. Clinical characteristics of 138 hospitalized patients with 2019 novel coronavirus–infected pneumonia in Wuhan, China. Jama. 2020;323(11):1061–1069.

21 Huang C, Wang Y, Li X, Ren L, Zhao J, Hu Y, et al. Clinical features of patients infected with 2019 novel coronavirus in Wuhan, China. The Lancet. 2020;395(10223):497–506.

22 Zhou F, Yu T, Du R, Fan G, Liu Y, Liu Z, et al. Clinical course and risk factors for mortality of adult inpatients with COVID-19 in Wuhan, China: a retrospective cohort study. The lancet. 2020;.

23 Guan Wj, Ni Zy, Hu Y, Liang Wh, Ou Cq, He Jx, et al. Clinical characteristics of 2019 novel coronavirus infection in China. MedRxiv. 2020;.

24 Henry BM, de Oliveira MHS, Benoit S, Plebani M, Lippi G. Hematologic, biochemical and immune biomarker abnormalities associated with severe illness and mortality in coronavirus disease 2019 (COVID-19): a meta-analysis. Clinical Chemistry and Laboratory Medicine (CCLM). 2020;1(ahead-of-print).

25 Guo T, Fan Y, Chen M, Wu X, Zhang L, He T, et al. Cardiovascular implications of fatal outcomes of patients with coronavirus disease 2019 (COVID-19). JAMA cardiology. 2020;.

26 Mercuro NJ, Yen CF, Shim DJ, Maher TR, McCoy CM, Zimetbaum PJ, et al. Risk of QT Interval Prolongation Associated With Use of Hydroxychloroquine With or Without Concomitant Azithromycin Among Hospitalized Patients Testing Positive for Coronavirus Disease 2019 (COVID-19). JAMA cardiology. 2020;.

27 Luo C, Wang K, Zhang H. Modelling the effects of chloroquine on KCNJ2-linked short QT syndrome. Oncotarget. 2017;8(63):106511.

28 Li X, Hu C, Su F, Dai J, et al. Hypokalemia and clinical implications in patients with coronavirus disease 2019 (COVID-19). MedRxiv. 2020;.

29 He J, Wu B, Chen Y, Tang J, Liu Q, Zhou S, et al. Characteristic ECG manifestations in patients with COVID-19. Canadian Journal of Cardiology. 2020;.

30 Gattinoni L, Coppola S, Cressoni M, Busana M, Rossi S, Chiumello D. Covid-19 does not lead to a "typical" acute respiratory distress syndrome. American journal of respiratory and critical care medicine. 2020;(ja).

31 Bennett CE, Anavekar NS, Gulati R, Singh M, Kane GC, Sandoval Y, et al. ST-segment Elevation, Myocardial Injury, and Suspected or Confirmed COVID-19 Patients: Diagnostic and Treatment Uncertainties. In: Mayo Clinic Proceedings. Elsevier; 2020. .

32 Ten Tusscher KH, Panfilov AV. Alternans and spiral breakup in a human ventricular tissue model. American Journal of Physiology-Heart and Circulatory Physiology. 2006;291(3):H1088–H1100.

33 Viswanathan PC, Rudy Y. Cellular arrhythmogenic effects of congenital and acquired long-QT syndrome in the heterogeneous myocardium. Circulation. 2000;101(10):1192–1198.

34 Antzelevitch C. Ionic, molecular, and cellular bases of QT-interval prolongation and torsade de pointes. Europace. 2007;9(suppl 4):iv4–iv15.

35 Shaw RM, Rudy Y. Electrophysiologic effects of acute myocardial ischemia: a theoretical study of altered cell excitability and action potential duration. Cardiovascular research. 1997;35(2):256–272.

36 Clayton RH. Re-entry in a model of ischaemic ventricular tissue. In: 2010 Computing in Cardiology. IEEE; 2010. p. 181–184.

37 Priya PK, Reddy MR. Study of factors affecting the progression and termination of drug induced torsade de pointes in two dimensional cardiac tissue. Journal of electrocardiology. 2017;50(3):332–341.

38 Gima K, Rudy Y. Ionic Current Basis of Electrocardiographic Waveforms A Model Study. Circulation Research. 2002;90(8):889–896.

39 Zipes RM. Mechanisms of sudden cardiac death. Journal of Clinical Investigation. 2005;115:2305–15.

40 Skogestad J, Aronsen JM. Hypokalemia-induced arrhythmias and heart failure: new insights and implications for therapy. Frontiers in physiology. 2018;9:1500.

41 Hanna EB, Glancy DL. ST-segment depression and T-wave inversion: classification, differential diagnosis, and caveats. Cleveland Clinic journal of medicine. 2011;78(6):404.

42 Waldo A. Prevalence and Prognostic Significance of Short QT Interval in a Middle-Aged Finnish Population Anttonen O, Junttila MJ, Rissanen H, et al (Päijät-Häme Central Hosp, Lahti, Finland; Natl Public Health Inst, Helsinki; Univ of Helsinki; et al) Circulation 116: 714-720, 2007. Year Book of Cardiology. 2008;2008:512–513.

43 Boris Rudic MB Rainer Schimpf. Short QT Syndrome – Review Of Diagnosis And Treatment. Arrhythmia & Electrophysiology Review. 2014;3:76–9.

44 Bryant SM, Wan X, Shipsey SJ, Hart G. Regional differences in the delayed rectifier current (I Kr and I Ks) contribute to the differences in action potential duration in basal left ventricular myocytes in guinea-pig. Cardiovascular research. 1998;40(2):322–331.

45 Rodriguez-Sinovas A, Cinca J, Tapias A, Armadans L, Tresanchez M, Soler-Soler J. Lack of evidence of M-cells in porcine left ventricular myocardium. Cardiovascular research. 1997;33(2):307–313.

46 Antzelevitch C. M cells in the human heart. Circulation research. 2010;106(5):815–817.

47 Glukhov AV, Fedorov VV, Lou Q, Ravikumar VK, Kalish PW, Schuessler RB, et al. Transmural Dispersion of Repolarization in Failing and Non Failing Human Ventricle. Circulation research. 2010;106(5):981.

48 Sweeney MO, Ruetz LL, Belk P, Mullen TJ, Johnson JW, Sheldon T. Bradycardia pacing-induced short-long-short sequences at the onset of ventricular tachyarrhythmias: a possible mechanism of proarrhythmia? Journal of the American College of Cardiology. 2007;50(7):614–622.

Table 3: Pseudo ECG parameters: T-peak and QT interval duration as a metric for assessing the effect of COVID-19, other comorbidities and in presence of HCQ

	QT interval (s)	T-peak (mV)
Control	0.345	0.2265
Mild COVID-19	0.325	0.152
Severe COVID-19	0.275	-0.170
Mild COVID-19 with HCQ	0.340	0.181
Severe COVID-19 with HCQ	0.275	-0.153
LQTS1	0.385	0.210
LQTS2	0.385	0.313
LQTS1 with HCQ	0.415	0.286
LQTS2 with HCQ	0.395	0.326
Hypokalemia1	0.355	0.229
Hypokalemia1 with HCQ	0.375	0.265
Hypokalemia2	0.380	0.217
Hypokalemia2 with HCQ	0.410	0.255
Hypokalemia3	0.390	0.210
Hypokalemia3 with HCQ	0.425	0.246
LQTS1 and Mild COVID-19	0.370	0.106, 0.096
LQTS1 and Mild COVID-19 with HCQ	0.390	0.158
LQTS1 and Severe COVID-19	0.295	-0.262
LQTS1 and Severe COVID-19 with HCQ	0.295	-0.238
LQTS2 and Mild COVID-19	0.375	0.245
LQTS2 and Mild COVID-19 with HCQ	0.375	0.252
LQTS2 and Severe COVID-19	0.300	0.015, -0.077
LQTS2 and Severe COVID-19 with HCQ	0.300	0.015, -0.087
Hypokalemia1a and Mild COVID-19	0.335	0.127, 0.153
Hypokalemia1 and Mild COVID-19 with HCQ	0.350	0.186
Hypokalemia1 and Severe COVID-19	0.285	-0.16, -0.087
Hypokalemia1 and Severe COVID-19 with HCQ	0.285	-0.14
Hypokalemia2 and Mild COVID-19	0.355	0.141
Hypokalemia2 and Mild COVID-19 with HCQ	0.38	0.174
Hypokalemia2 and Severe COVID-19	0.300	-0.156
Hypokalemia2 and Severe COVID-19 with HCQ	0.305	-0.126
Hypokalemia3 and Mild COVID-19	0.365	0.133
Hypokalemia3 and Mild COVID-19 with HCQ	0.395	0.168
Hypokalemia3 and Severe COVID-19	0.31	-0.155
Hypokalemia3 and Severe COVID-19 with HCQ	0.32	-0.121